

1 **Optimizing *E. coli* as a formatotrophic platform for bioproduction via the**  
2 **reductive glycine pathway**

3 Seohyoung Kim<sup>1</sup>, Néstor David Giraldo<sup>1</sup>, Vittorio Rainaldi<sup>1</sup>, Fabian Machens<sup>1</sup>, Florent Collas<sup>2</sup>, Armin  
4 Kubis<sup>2</sup>, Frank Kensy<sup>2</sup>, Arren Bar-Even<sup>1,†</sup>, Steffen N. Lindner<sup>1,3,\*</sup>

5

6 <sup>1</sup>Max Planck Institute of Molecular Plant Physiology, Am Mühlenberg 1, 14476 Potsdam-Golm,  
7 Germany

8 <sup>2</sup>b.fab GmbH, Gottfried-Hagen-Straße 60, 51105 Köln, Germany

9 <sup>3</sup>Department of Biochemistry, Charité – Universitätsmedizin Berlin, Charitéplatz 1, 10117 Berlin,  
10 Germany

11 <sup>†</sup>Deceased

12 \* Corresponding author: [steffen.lindner@charite.de](mailto:steffen.lindner@charite.de)

13

14 **Abstract**

15 Microbial C1 fixation has a vast potential to support a sustainable circular economy. Hence, several  
16 biotechnologically important microorganisms have been recently engineered for fixing C1 substrates.  
17 However, reports about C1-based bioproduction with these organisms are scarce. Here, we describe  
18 the optimization of a previously engineered formatotrophic *Escherichia coli* strain. Short-term adaptive  
19 laboratory evolution enhanced biomass yield and accelerated growth of formatotrophic *E. coli* to 3.3  
20 g-CDW/mol-formate and 6 hours doubling time, respectively. Genome sequence analysis revealed  
21 that manipulation of acetate metabolism is the reason for better growth performance, verified by  
22 subsequent reverse engineering of the parental *E. coli* strain. Moreover, the improved strain is  
23 capable of growing to an OD<sub>600</sub> of 22 in bioreactor fed-batch experiments, highlighting its potential use  
24 for industrial bioprocesses. Finally, demonstrating the strain's potential to support a sustainable,  
25 formate-based bioeconomy, lactate production from formate and CO<sub>2</sub> was engineered. The optimized  
26 strain generated 1.2 mM lactate—10 % of the theoretical maximum—providing the first proof-of-  
27 concept application of the reductive glycine pathway for bioproduction.

28

29

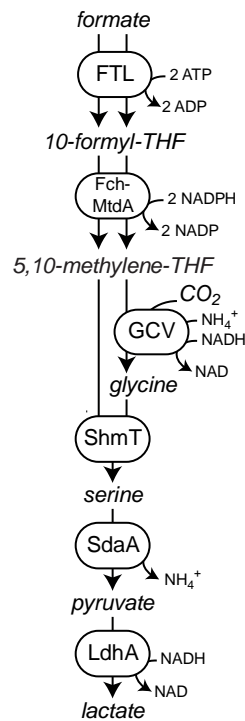
## 30 **Introduction**

31 The valorization of carbon dioxide is a major challenge in our society and is subject to intense  
32 research and investment. Naturally, the biological transformation of carbon dioxide takes place in  
33 plants and algae on a massive scale. However, photosynthetic carbon fixation greatly suffers from  
34 low-energy conversion efficiencies in the range of 3–5% (Janssen et al., 2003; Zhu et al., 2010). Pure  
35 chemical transformation, where various chemicals such as urea, methanol, and salicylic acid can be  
36 derived directly from carbon dioxide, might be another option (He et al., 2013; Wong, 2014). However,  
37 such processes rely on extreme conditions and suffer from a limited product spectrum and low  
38 product selectivity. An emerging solution is to integrate biological and chemical processes to combine  
39 their individual strengths and circumvent their weaknesses. In such an approach, carbon dioxide can  
40 be reduced electrochemically, using a renewable energy source such as solar or wind, to various C1  
41 compounds. Among them is formic acid, which can be produced with a very high faradaic efficiency  
42 and can be utilized as a feedstock for microorganisms (Chong et al., 2016; Han et al., 2012; Yishai et  
43 al., 2016). Formic acid is one of the most suitable C1 compounds for the bioindustry, especially  
44 because of its solubility and low toxicity (Claassens et al., 2019).

45 However, engineering natural C1-assimilating microorganisms to produce value-added biochemicals  
46 from single-carbon compounds is often limited by their poor growth characteristics and recalcitrance  
47 to genetic modification. Various natural C1 assimilation routes have been identified, including the  
48 reductive pentose phosphate cycle, the reductive acetyl-CoA pathway, and the reductive citric acid  
49 cycle from various domains of life (Bar-Even et al., 2012; Bar-Even et al., 2012; Berg et al., 2010).  
50 Nature has optimized these microorganisms, enzymes, and metabolic fluxes over billions of years,  
51 rendering attempts to improve energy consumption and carbon-fixation efficiency very challenging.  
52 Implementing natural or new-to-nature synthetic pathways for C1 assimilation into biotechnologically  
53 important microbes such as *E. coli*, which do not naturally grow on C1 compounds, can solve these  
54 problems. Assimilation of C1 compounds such as CO<sub>2</sub>, formate, CO, or methanol via their respective  
55 assimilation pathways has been receiving increased attention (Bang et al., 2020; Chen et al., 2020;  
56 Gassler et al., 2020; Gleizer et al., 2019; Meyer et al., 2018; Schwander et al., 2016). Besides the  
57 reductive acetyl-CoA pathway, the synthetic and oxygen-tolerant reductive glycine (rGly) pathway is  
58 the most efficient formate assimilation pathway (Bar-Even et al., 2013; Claassens et al., 2022). This

59 pathway was recently successfully engineered in *E. coli* for generation of all biomass from formate  
60 and CO<sub>2</sub> (Figure 1), reaching a doubling time of 9 h and a biomass yield of 2.3 g cell dry weight / mol  
61 (CDW/mol) formate (Kim et al., 2020). However, so far bioproduction via synthetic C1-assimilation  
62 pathways has not been reported.

63 In this work, growth performance of the formatotrophic *E. coli* strain was improved using an adaptive  
64 laboratory evolution approach on formate under 10% CO<sub>2</sub> atmosphere. Genome sequencing identified  
65 mutations that apparently increased the growth performance on formate, and their effects were  
66 verified through reverse engineering. Finally, we demonstrate high biomass production in a fed-batch  
67 experiment and engineer lactate production from formate by an optimized *E. coli* strain.



68

69 **Figure 1. Reductive glycine pathway as operating in the formatotrophic *E. coli* strain.** Displayed is formate  
70 and CO<sub>2</sub> conversion to lactate as a final bioproduction product.

71

72

## 73 **Materials and methods**

### 74 **Chemicals and reagents**

75 Primers were synthesized by Integrated DNA Technologies (IDT, Leuven, Belgium). PCR reactions  
76 were carried out either using Phusion High-Fidelity DNA Polymerase or Dream Taq (Thermo Fisher  
77 Scientific, Dreieich, Germany). Restrictions and ligations were performed using FastDigest enzymes  
78 and T4 DNA ligase, respectively, all purchased from Thermo Fisher Scientific. Sodium formate was  
79 ordered from Sigma-Aldrich (Steinheim, Germany).  $^{13}\text{CO}_2$  was obtained from Cambridge Isotope  
80 Laboratories (Andover, MA, USA).

81

### 82 **Bacterial strains**

83 Wild-type *Escherichia coli* strain MG1655 ( $F^- \lambda^- ilvG^- rfb-50 rph-1$ ) was used as the host for all genetic  
84 modifications. *E. coli* strains DH5 $\alpha$  ( $F^- \lambda^- \Phi 80lacZ\Delta M15 \Delta(lacZYA-argF)U169 deoR, recA1 endA1,$   
85  $hsdR17(rK^- mK^+) phoA supE44 thi-1 gyrA96 relA1$ ) and ST18 ( $pro thi hsdR^+ T_p^r Sm^r$ ;  
86 chromosome::RP4-2 Tc::Mu-Kan::Tn7 $\lambda pir\Delta hemA$ ) were used for cloning and conjugation procedures,  
87 respectively. A formatotrophic *E. coli* strain equipped with a reductive glycine pathway (K4e) (Kim et  
88 al., 2020) was used as base strain for adaptive evolution and reverse engineering. All strains are  
89 listed in Table 1.

90

### 91 **Genome engineering**

92 Gene knockouts were introduced in MG1655 by P1 phage transduction (Thomason et al., 2007).  
93 Single-gene knockout mutants from the National BioResource Project (NIG, Japan) (Baba et al., 2006)  
94 were used as donors of specific mutations. For the recycling of selection markers (as the multiple-  
95 gene deletions and integrations required), all antibiotic cassettes integrated into the genome were  
96 flanked by FRT (flippase recognition target) sites. Cells were transformed with a flippase recombinase  
97 helper plasmid (FLPe, replicating at 30°C; Gene Bridges, Heidelberg, Germany) carrying a gene  
98 encoding FLP which recombines at the FRT sites and removes the antibiotic cassette. Elevated  
99 temperature (37°C) was subsequently used to cure the cells from the FLPe plasmid.

100

### 101 **Synthetic-operon construction**

102 A gene native to *E. coli*, lactate dehydrogenase (*ldhA*), was prepared via PCR amplification from the *E.*  
103 *coli* MG1655 genome. The PCR product was integrated into a high-copy-number cloning vector pNiv  
104 to construct synthetic operons using a method described previously (Zelcbuch et al., 2013). Plasmid-  
105 based gene overexpression was achieved by cloning the desired synthetic operon into a pZ vector  
106 (15A origin of replication, streptomycin marker) digested with EcoRI and PstI, utilizing T4 DNA ligase.  
107 Promoters and ribosome binding sites were used as described previously (Braatsch et al., 2008;  
108 Zelcbuch et al., 2013).

109

### 110 **Growth medium and conditions**

111 LB medium (1% NaCl, 0.5% yeast extract, 1% tryptone) was used for strain propagation. Further  
112 cultivation was done in M9 minimal media (50 mM Na<sub>2</sub>HPO<sub>4</sub>, 20 mM KH<sub>2</sub>PO<sub>4</sub>, 1 mM NaCl, 20 mM  
113 NH<sub>4</sub>Cl, 2 mM MgSO<sub>4</sub>, and 100 μM CaCl<sub>2</sub>) with trace elements (134 μM EDTA, 13 μM FeCl<sub>3</sub>·6 H<sub>2</sub>O, 6.2  
114 μM ZnCl<sub>2</sub>, 0.76 μM CuCl<sub>2</sub>·2 H<sub>2</sub>O, 0.42 μM CoCl<sub>2</sub>·2 H<sub>2</sub>O, 1.62 μM H<sub>3</sub>BO<sub>3</sub>, 0.081 μM MnCl<sub>2</sub>·4 H<sub>2</sub>O). For  
115 the cell-growth test, overnight cultures in LB medium were used to inoculate a pre-culture at an optical  
116 density (600 nm, OD<sub>600</sub>) of 0.02 in 4 ml fresh M9 medium containing 10 mM glucose, 1 mM glycine,  
117 and 30 mM formate in 10-ml glass test tubes. Cells were then cultivated at 37°C and shaking at 240  
118 rpm. Cell cultures were harvested by centrifugation (18,407 × g, 3 min, 4°C), washed twice with fresh  
119 M9 medium, and used to inoculate the main culture, conducted aerobically either in a 10-ml glass  
120 tube or in Nunc 96-well microplates (Thermo Fisher Scientific) with appropriate carbon sources  
121 according to strain and specific experiment. In the microtiter-plate cultivations each well contained  
122 150 μl culture covered with 50 μl mineral oil (Sigma-Aldrich) to avoid evaporation. Growth  
123 experiments were conducted (either at 100% air or 90% air / 10% CO<sub>2</sub>) in a BioTek Epoch 2 plate  
124 reader (Agilent, Santa Clara, CA, USA) at 37°C. Growth (OD<sub>600</sub>) was measured after a kinetic cycle of  
125 12 shaking steps, which alternated between linear and orbital (1 mm amplitude) and were each 60 s  
126 long. OD<sub>600</sub> values measured in the plate reader were calibrated to represent OD<sub>600</sub> values in  
127 standard cuvettes according to OD<sub>cuvette</sub> = OD<sub>plate</sub> / 0.23. Glass-tube cultures were carried out in 4 ml

128 of working volume, at 37°C and shaking at 240 rpm. Volume loss due to evaporation was  
129 compensated by adding the appropriate amount of sterile double-distilled water (ddH<sub>2</sub>O) to the culture  
130 tubes every two days. All growth experiments were performed in triplicate, and the growth curves  
131 shown represent the average.

132

### 133 **Lactate production experiments**

134 Colonies from LB plates for starting liquid cultures in test tubes in LB were incubated at 37°C  
135 overnight. All strains grown overnight were washed 3 times with minimal M9 medium. Each strain was  
136 then inoculated in test tubes with starting OD<sub>600</sub> of ~ 0.05. All tubes were incubated in an orbital  
137 shaker at 37°C with 10% CO<sub>2</sub> until the stationary phase in each treatment was reached. Selected  
138 cultures were fed with formic acid when each culture reached the stationary phase (OD stopped  
139 increasing). Formic acid was added to each tube to increase its concentration by either 30 mM or 60  
140 mM. For each strain, control tubes were left without feeding. Expression of *ldhA* was induced by  
141 addition of isopropyl β-d-1-thiogalactopyranoside (IPTG; 1 mM final) together with formic acid.  
142 Periodic sampling was performed for measuring the extracellular ions dissolved in the medium by ion  
143 chromatography (Dionex ICS 6000 HPAEC, IonPac AS11-HC-4μm Analytical/Capillary Column;  
144 Thermo Fisher Scientific). At each sampling point, 200 μl were taken from the cultures and centrifuged  
145 at 15,000 rpm for 3 min. The supernatant was then diluted 20 times with ddH<sub>2</sub>O. The diluted sample  
146 was centrifuged again at 15,000 rpm for 3 min and transferred to a chromatography vial for the ion  
147 chromatography analysis.

148

### 149 **Dry-weight analysis**

150 To determine dry cell weight of *E. coli* grown on formate or methanol, pre-cultures prepared as  
151 described above were inoculated to a final OD<sub>600</sub> of 0.01 into fresh M9 medium containing 90 mM of  
152 formate in a 125-ml pyrex Erlenmeyer flask and grown at 37°C with shaking at 240 rpm. Up to 50 ml  
153 of cell culture growing in shake flasks were harvested by centrifugation (3,220 × g, 20 min). To  
154 remove residual medium compounds, cells were washed using three cycles of centrifugation (7,000 ×  
155 g, 5 min) and resuspension in 2 ml ddH<sub>2</sub>O. Cell solutions were transferred to a pre-weighed and pre-

156 dried aluminum dish and dried at 90 °C for 16 h. The weight of the dried cells in the dish was  
 157 determined and subtracted by the weight of the empty dish. Cell dry weight (CDW) of *E. coli* strains  
 158 was measured during exponential growth phase (OD<sub>600</sub> of 0.6–0.8) in the presence of 10% CO<sub>2</sub> on 90  
 159 mM formate.

160 Table 1. Strains and plasmids used in this study

Strain/plasmid	Description/genotype	Source
<b>Strains</b>		
MG1655	F <sup>-</sup> λ <sup>-</sup> <i>ilvG</i> <sup>-</sup> <i>rfb-50 rph-1</i>	(Blattner et al., 1997)
DH5α	F <sup>-</sup> λ <sup>-</sup> Φ80 <i>lacZ</i> ΔM15 Δ( <i>lacZYA-argF</i> )U169 <i>deoR recA1 endA1 hsdR17</i> (rK <sup>-</sup> mK <sup>+</sup> ) <i>phoA supE44 thi-1 gyrA96 relA1</i>	(Meselson and Yuan, 1968)
ST18	<i>pro thi hsdR</i> <sup>+</sup> T <sub>p</sub> <sup>f</sup> Sm <sup>r</sup> ; chromosome::RP4-2 Tc::Mu-Kan::Tn7/λpir Δ <i>hemA</i>	(Thoma and Schobert, 2009)
SerAux	MG1655, Δ <i>serA</i> Δ <i>ltaE</i> Δ <i>kbl</i> Δ <i>aceA</i>	(Yishai et al., 2018)
gC <sub>1</sub> M gC <sub>2</sub> M gC <sub>3</sub> M gEM (K4)	gC <sub>1</sub> M gC <sub>2</sub> M gC <sub>3</sub> M, ss10-P <sub>STRONG</sub> -RBS <sub>A</sub> - <i>fdh</i>	(Kim et al., 2020)
K4e	K4, <i>pntA</i> <sup>*</sup> , <i>fdh</i> <sup>*</sup>	(Kim et al., 2020)
K4e, g- <i>pdhR</i> <sup>*</sup> , g- <i>ackA</i> <sup>*</sup> (K4e2)	K4e strain with a nonsense mutation (E239X) in <i>pdhR</i> and mobile element insertion in the promoter region of <i>ackA</i>	This study
K4e Δ <i>ackA-pta</i>	K4e, Δ <i>ackA</i> Δ <i>pta</i>	This study
K4e2 Δ <i>ackA-pta</i>	K4e2, Δ <i>ackA</i> Δ <i>pta</i>	This study
KS44	K4e Δ <i>ackA</i> Δ <i>pta</i> Δ <i>dld</i>	This study
<b>Plasmids</b>		
pSStac	Overexpression plasmid with p15A origin, streptomycin resistance, tac promoter	This study
pSStac- <i>ldhA</i>	pSStac backbone for overexpression of <i>ldhA</i> from <i>E. coli</i>	This study

161

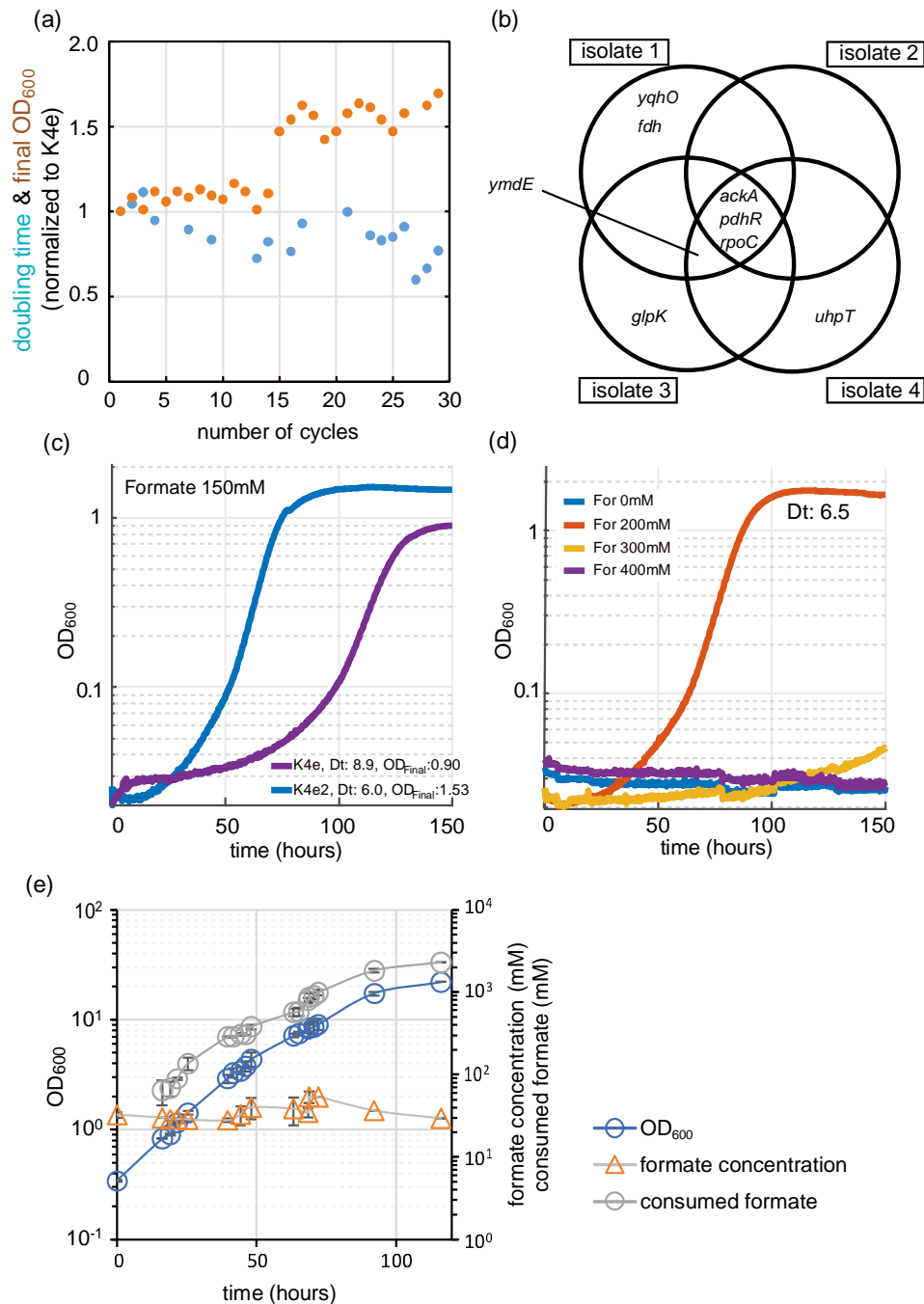
162

## 163 **Results and discussion**

### 164 **Adaptive laboratory evolution leads to improved formatotrophic growth characteristics**

165 We previously developed a formatotrophic *E. coli* strain named K4e (Kim et al., 2020). Engineering of  
166 this strain was achieved following a modular strategy that included four different modules: (i) a C<sub>1</sub>  
167 module, consisting of formate THF ligase, methenyl-THF cyclohydrolase, and methylene-THF  
168 dehydrogenase, all from *Methylobacterium extorquens*, together converting formate into methylene-  
169 THF; (ii) a C<sub>2</sub> module, consisting of the endogenous enzymes of the glycine cleavage system (GCS,  
170 GcvT, GcvH, and GcvP), which condenses methylene-THF with CO<sub>2</sub> and ammonia to give glycine; (iii)  
171 a C<sub>3</sub> module, consisting of serine hydroxymethyltransferase (SHMT) and serine deaminase, together  
172 condensing glycine with another methylene-THF to generate serine and finally pyruvate; and (iv) an  
173 energy module, which consists of formate dehydrogenase (FDH) from *Pseudomonas sp.* (strain 101),  
174 generating reducing power and energy from formate (Kim et al., 2020). After initial growth was  
175 observed, the strain's growth was optimized, reaching performance characteristics of isolated mutants  
176 (K4e) of 9 h doubling time and a biomass yield of 2.3 g CDW/mol formate. Subsequent genome  
177 sequence analysis and reverse engineering revealed that upregulation mutations in the energy  
178 module and the membrane-bound transhydrogenase (a gene product of *pntAB*) supported enhanced  
179 growth on formate.





180

181 **Figure 2. Evolution approaches for enhancing growth on formate.** (a) Evolution from K4e to K4e2 via  
 182 laboratory evolution was conducted in test tubes in M9 minimal medium with 90 mM formate in the presence of  
 183 10% CO<sub>2</sub>. Final OD<sub>600</sub> (orange circle) and doubling times (blue circle) were normalized to K4e. (b) All identified  
 184 mutated genes obtained after 30 cycles of re-inoculation. Only newly identified mutations are shown compared  
 185 with parental strain K4e. (c) Growth profile comparison between evolved strains. (d) Formate tolerance test of  
 186 K4e2. (e) Fed-batch cultivation of strain K4e2 in a bioreactor with pH control. Feeding and pH control were  
 187 achieved by pumping 10 M of formic acid. List of genes: *pdhR*, pyruvate dehydrogenase complex regulator;  
 188 *ymdE*, uncharacterized protein; *ackA*, acetate kinase; *yqhO*, biofilm formation related gene; *rpoC*, RNA  
 189 polymerase subunit beta; *glpK*, glycerol kinase; Experiments (c) and (d) were conducted at 10% CO<sub>2</sub> in 96-well  
 190 plates and were performed in triplicates, which displayed identical growth curves ( $\pm$  5%) and hence were  
 191 averaged. The corresponding doubling times (Dt) are shown in the figure.

192

193 To improve K4e's growth performance further, we used this strain in an adaptive laboratory evolution  
194 (ALE) experiment, selecting for faster growth on formate and CO<sub>2</sub>. The cells were grown in M9  
195 minimal medium containing formate and CO<sub>2</sub> as the sole carbon sources. We cultivated the K4e strain  
196 in test tubes with a formate concentration of 90 mM in a CO<sub>2</sub> atmosphere set to 10%. Once the  
197 turbidity reached an OD<sub>600</sub> of 1.0, the culture was diluted 1:100 into fresh medium of the same  
198 composition to start a new cultivation cycle. While the doubling time gradually decreased over 30  
199 cycles, the final OD<sub>600</sub> was stagnant for the first 14 cycles (≤ 90 generations). From cycle 15 onwards  
200 it appeared that a new mutant became dominant and a stairway-like enhancement in OD<sub>600</sub> was  
201 observed (Figure 2a). To confirm the growth improvement of individuals from the ALE culture, growth  
202 of four independent isolates (originating from cycle 26) was analyzed in the plate reader. These  
203 independent growth tests conducted with the newly isolated strains, named as 'K4e2', confirmed > 40%  
204 faster growth of the isolates, reflected by a decrease in doubling time from 9 h to 6.3 h. Strikingly, the  
205 isolates also showed a 40% increase in biomass yield, from 2.3 to 3.3 g-CDW/mol formate.  
206 Furthermore, increased tolerance toward formate was observed for the newly isolated strain K4e2,  
207 which showed accelerated growth as expressed by a reduced doubling time from 8.9 to 6 h and an  
208 increase of the final OD<sub>600</sub> from 0.9 to 1.53 at 150 mM formate (Figure 2c). Moreover, even with 200  
209 mM of formate, the strain grows normally without any significant growth-rate reduction (6.5 h doubling  
210 time). Compared to K4e, which showed optimal growth at < 90 mM formate and poor growth at > 150  
211 mM, K4e2 represents a clear improvement. Thus, the isolated strain not only improved biomass  
212 productivity, but also in formate tolerance, a feature that is especially beneficial in terms of bioprocess  
213 design, since the system can be more robust with strains that exhibit higher formate tolerance.

214 To reveal the genetic changes underlying the growth improvements of the K4e2 isolates, the genomes  
215 of all four isolates were sequenced (see supplementary table for all mutations identified). The analysis  
216 revealed that all four isolates share three common mutations. The first mutation is a mobile element  
217 insertion in the promoter region of *ackA*, which encodes an acetate kinase, responsible for acetate  
218 uptake or acetate overflow metabolism in the presence of oxygen (Szenk et al., 2017; Wolfe, 2005).  
219 The second mutation is a nonsense mutation (E239X) in *pdhR*, encoding a DNA-binding  
220 transcriptional dual regulator. The gene product of *pdhR* represses genes of the pyruvate

221 dehydrogenase complex (PDH) and in the terminal electron transport systems (Ogasawara et al.,  
222 2007). As PDH converts pyruvate—a product of formate assimilation via the rGly pathway—to acetyl-  
223 CoA, a change in gene expression brought about by a *pdhR* mutation might positively influence  
224 growth by decreasing oxidative flux via the TCA cycle. Moreover, the enzyme complexes of PDH and  
225 GCS, the key enzyme of the rGly pathway, both contain lipoamide dehydrogenase, the expression of  
226 the corresponding gene (*lpd*) is repressed by PdhR (Quail and Guest, 1995). Lastly, a point mutation  
227 (A919V) occurs at *rpoC*, which encodes RNA polymerase subunit  $\beta'$ . Here, a direct relevance to  
228 carbon and energy metabolism is not obvious (Figure 2b).

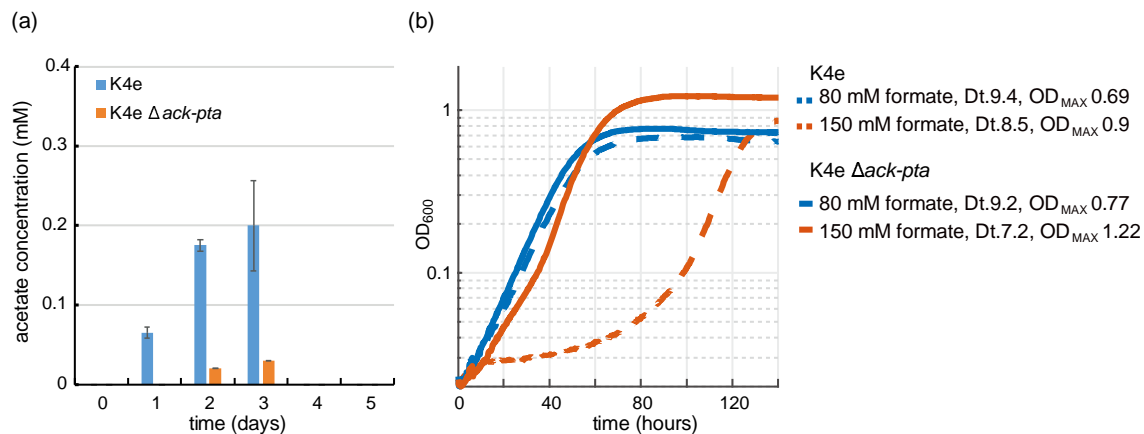
229

### 230 **Blocking of acetate overflow metabolism improves formatotrophic growth**

231 Among the mutations found in the K4e2 isolates from the evolution experiment, the mobile element  
232 (ME) insertion into the upstream region of *ackA* (acetate kinase) provides important information  
233 regarding the formatotrophic growth mode of *E. coli* via the rGly pathway. The ME insertion occurred  
234 at the -35 element in the promoter region of *ackA*, which we assume would decrease the level of  
235 *ackA* expression. It is not intuitive to consider the occurrence of acetate overflow metabolism in *E. coli*  
236 while growing on formate and reaching only very limited final OD<sub>600</sub> (Basan et al., 2015; Bernal et al.,  
237 2016). However, the observed ME insertion suggests that by-product generation might be a limiting  
238 factor while growing on formate. Hence, we measured accumulation of metabolites, including acetate,  
239 succinate, lactate, and pyruvate during formatotrophic growth. Acetate accumulation was indeed  
240 observed from an early growth stage and reached up to 0.2 mM in K4e (Figure 3a). We found that the  
241 excreted acetate is re-assimilated as the cell enters the mid-exponential phase. This can be facilitated  
242 by either acetate kinase (*ackA*) and phosphotransacetylase (*pta*), consuming one ATP, or acetyl-CoA  
243 synthetase (*acs*), which converts acetate to acetyl-CoA while consuming two ATP equivalents (Kumari  
244 et al., 1995). In order to prevent K4e from synthesizing acetate, causing loss of carbon and energy,  
245 and to mimic the ME insertion found in the K4e2 isolates, both *ackA* and *pta* were deleted, resulting in  
246 the K4e $\Delta$ *ackA-pta* strain. When K4e $\Delta$ *ackA-pta* was cultured using the same conditions, acetate  
247 excretion was strongly reduced. To compare the growth performance of K4e and K4e $\Delta$ *ackA-pta*, two  
248 different formate concentrations were used. With 80 mM formate, both strains show similar growth  
249 patterns with almost identical doubling times. However, with 150 mM formate, the K4e $\Delta$ *ackA-pta*

250 strain displays not only a reduced doubling time of 7.2 h (as compared to 8.5 h of K4e), but also  
251 exhibits a 30% increase in the final OD<sub>600</sub> (Figure 3b). Indeed, we determined the observed biomass  
252 yield of K4eΔ*ackA-pta* to be 3.1 g CDW/mol formate, close to that of K4e2 (3.3 g CDW/mol formate).  
253 Moreover, the apparent lag phase of K4e on 150 mM formate was not present in K4eΔ*ackA-pta*, thus  
254 the K4eΔ*ackA-pta* strain grew within 80 h to the stationary phase, while the parental strain required  
255 more than 140 h to reach the stationary phase. It is unclear how blocking of the acetate overflow  
256 metabolism leads to increased formate tolerance. It is conceivable that the complete oxidation of  
257 acetyl-CoA via the tricarboxylic cycle provides additional energy to deal with toxicity exerted by  
258 formate. Thus, abolishing acetate biosynthesis in K4e is apparently helpful for growth on formate.

259



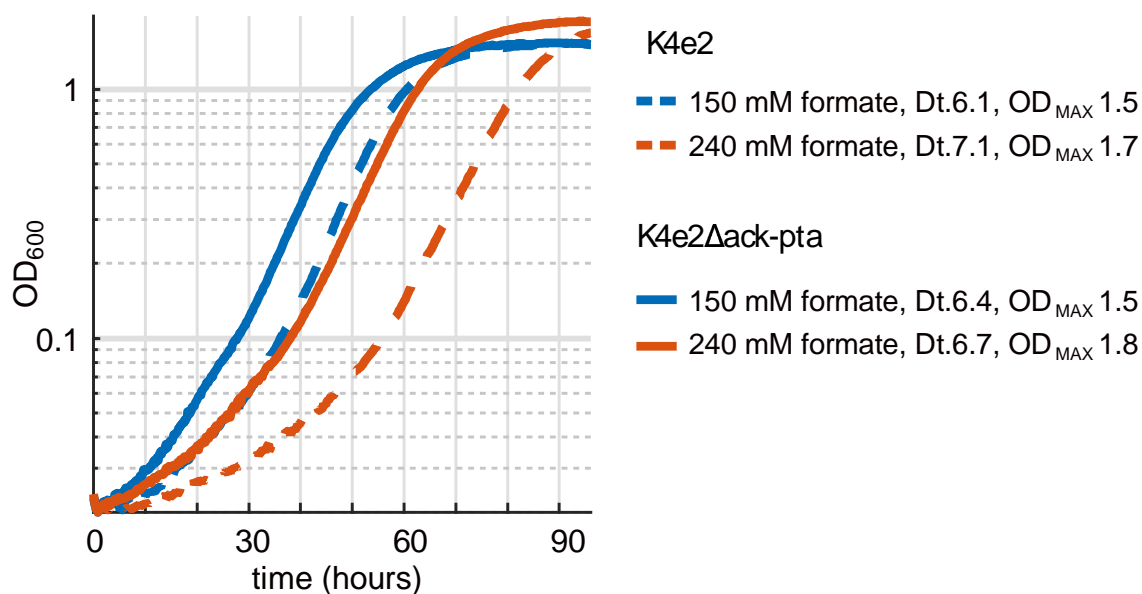
260

261 **Figure 3. Effect of acetate overflow metabolism on the growth of K4e.** (a) Acetate accumulation of K4e in  
262 test tubes with 90 mM initial formate. Only acetate was excreted in K4e and re-assimilated as the cell growth  
263 enters exponential phase. Strongly reduced acetate production was observed with K4e Δ*ackA-pta*. (b) Growth  
264 profile of K4e and K4eΔ*ackA-pta* on 80 and 150 mM formate in 96-well plate experiments performed in triplicates,  
265 which displayed identical growth curves ( $\pm 5\%$ ). Deletion of *ack-pta* resulted in increasing final OD<sub>600</sub> and high  
266 formate tolerance. Dt, doubling time.

267

268 To further investigate if a complete deletion of *ackA* and *pta* in the evolved K4e2 strain would  
269 positively influence the strain's growth performance, we deleted both genes in the K4e2 strain,  
270 yielding K4e2Δ*ackA-pta*. A direct comparison of growth of K4e2 to K4e2Δ*ackA-pta* revealed no  
271 difference in terms of doubling times and final OD<sub>600</sub> when strains grew with 150 or 240 mM formate  
272 (Figure 4). However, K4e2Δ*ackA-pta* clearly displays a reduced lag phase before the onset of  
273 exponential growth, suggesting that the complete deletions allow the strain to use the formate more  
274 efficiently. However, this is not reflected in the observed biomass yield of 3.4 g CDW/mol formate,

275 which is virtually identical to the biomass yield of the parental strain K4e2. However, the biomass  
276 yields achieved by K4e2 exceeds the reported average biomass yields of microorganisms naturally  
277 growing on formate via the Calvin–Benson–Basham cycle (3.2 g CDW/mol formate) (Claassens et al.,  
278 2019).



279

280 **Figure 4: Deletion of *ack-pta* in K4e2 further optimizes formatotrophic growth.**

281

## 282 **Fed-batch cultivation for high biomass generation**

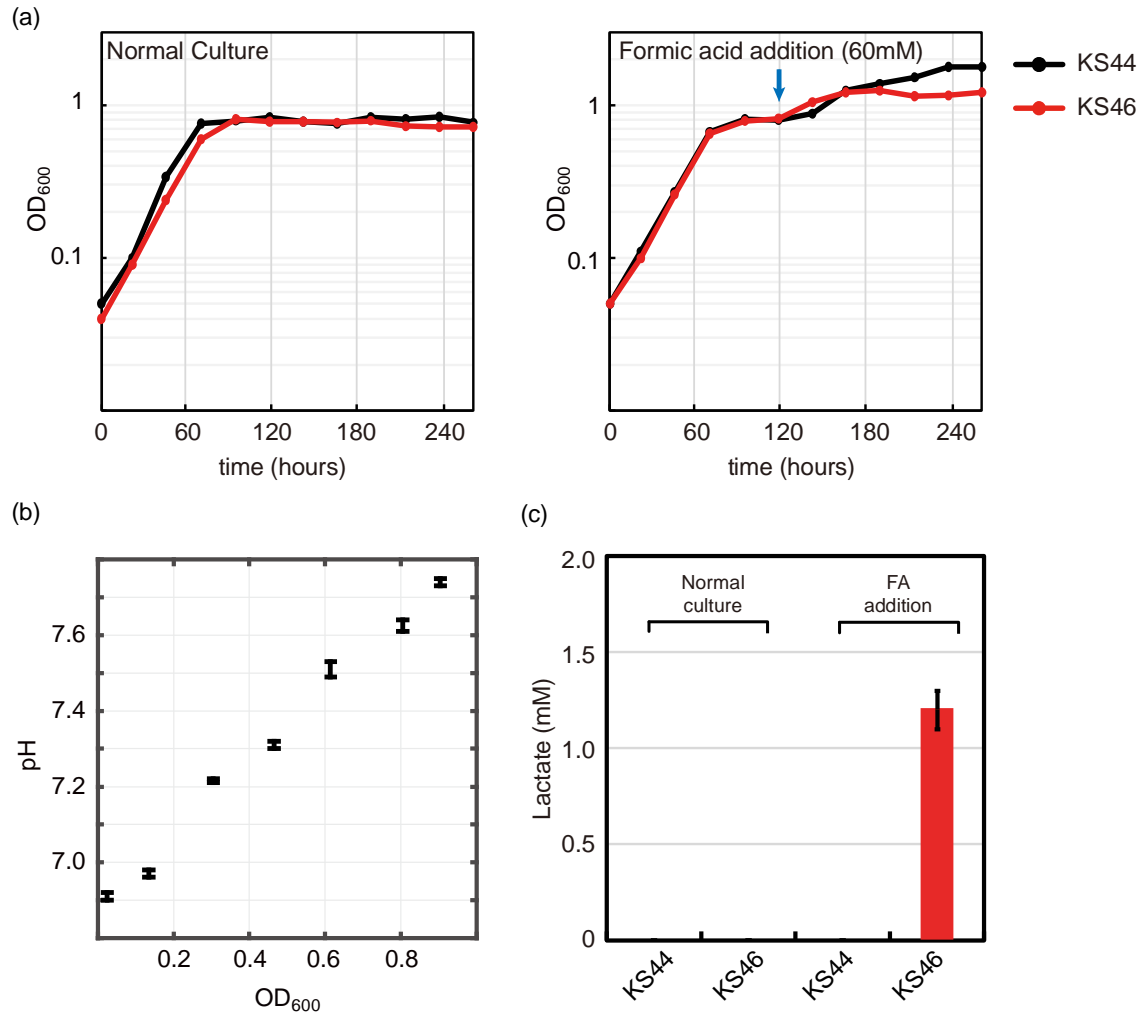
283 In order to characterize the strain's potential for large-scale production we conducted fed-batch  
284 cultivation in a 1-l stirred-tank bioreactor, growing strain K4e2 in M9 medium with 30 mM formate at  
285 pH 7. Control of pH and feeding of formate was done using 10 M formic acid. Starting from an  
286 inoculation OD<sub>600</sub> of 0.34, the strain reached a final OD<sub>600</sub> of 22 within 116 h (corresponding to 6  
287 doublings) of incubation with a growth rate of 0.048 h<sup>-1</sup>, corresponding to a doubling time of 14.4 h.  
288 The total biomass produced corresponded to 8 g CDW/l (Figure 2e). With a total consumption of  
289 2.289 mol/l formate, the observed biomass yield was determined to be 3.5 g CDW/mol formate, which  
290 is consistent with the values derived from batch cultivations. The achieved cell density and growth  
291 velocity largely exceeds those previously reported for engineered formatotrophic *E. coli* (Bang et al.,  
292 2020). This highlights the potential of the engineered strain for use in industrial bioprocesses, where  
293 high cell densities are often required to achieve economic feasibility. However, some improvement

294 with respect to biomass yield and doubling time is still possible, especially when comparing to the  
295 reported maximal theoretical biomass yields of ~ 5 g CDW/mol formate (Bar-Even et al., 2013; Cotton  
296 et al., 2020). We thus set out to further improve our strains by analyzing and making use of mutations  
297 that accumulated during the adaptive evolution.

298

### 299 **Formatrophic lactate production in *E. coli***

300 Lactate was selected as a proxy chemical to show the potential of formatrophic bioproduction.  
301 Lactate is an important chemical used in the food and chemical industries as it has a hydroxyl and a  
302 carboxyl functional group and can undergo self-esterification to form poly-lactic acid (PLA), a well-  
303 known polymer for producing bio-plastic (Maki-Arvela et al., 2014). Lactate can be generated by a  
304 reaction catalyzed by lactate dehydrogenase (*ldhA*), which oxidizes NADH using pyruvate as an  
305 electron acceptor. In order to prevent *E. coli* from re-assimilating the lactate, quinone dependent D-  
306 lactate dehydrogenase (*dld*) was deleted, generating K4e $\Delta$ *ackA-pta* $\Delta$ *dld*, named KS44. To achieve  
307 formatrophic lactate production, the KS44 strain was transformed with the *ldhA* gene cloned into an  
308 IPTG-inducible expression cassette in plasmid pSStac. The final strain with *ldhA* overexpression was  
309 named KS46. To test for IPTG-inducible lactate production from formate, we applied a two-phased  
310 fed-batch strategy. The growth phase was started in 90 mM formate and continued until the cells  
311 entered the stationary phase. The production phase was initiated by adding 1 mM IPTG and 60 mM of  
312 formic acid to the culture (Figure 5a). During the growth phase, the pH of the culture increases due to  
313 formate uptake into the cell, either via a proton symport mechanism or in the form of free formic acid  
314 (Wang et al., 2009; Wei et al., 2011; Wiechert and Beitz, 2017). Assimilation of 90 mM formate  
315 increased the culture pH from 6.9 to 7.8 (Figure 5b). Addition of 60 mM formic acid decreased the  
316 culture's pH back from 7.8 to 6.9. Along with the two-phased fed-batch strategy, a normal batch  
317 culture was also cultivated for comparison. However, we were able to detect lactate production only in  
318 the fed-batch cultivation (1.2 mM; Figure 5c), corresponding to almost 10% of the maximal theoretical  
319 yield (Cotton et al., 2020).



320

321 **Figure 5. Lactate production from formate with formatotrophic *E. coli*.** (a) Engineered *E. coli*  
322 strain was cultured in minimal medium using 90 mM formate and 10% CO<sub>2</sub> as carbon sources. Two  
323 different cultivation methods were tested: normal batch mode and fed-batch mode with the addition of  
324 60 mM formic acid (FA) at the indicated time point. (b) pH profile during growth on formate. Cell  
325 growth on formate directly correlates with increased medium pH due to the accumulation of OH<sup>-</sup>. (c)  
326 Lactate production was observed only with the strain in the fed-batch mode along with *ldhA*  
327 overexpression (n = 4, lactate measurement was conducted at the end of cultivation).

328

329

330

331

332

### 333 **Conclusion**

334 This study demonstrates that a previously engineered formatotrophic *E. coli* strain equipped with the  
335 rGly pathway can be optimized for the production of value-added chemicals such as lactate. Adaptive  
336 laboratory evolution conducted with CO<sub>2</sub> and formate as carbon sources yielded a strain with  
337 increased biomass yield, shorter doubling time, and the ability to grow to high cellular densities.  
338 Interestingly, formate tolerance was increased as well, allowing growth with 200 mM formate, while  
339 the parent formatotrophic strain K4e did not grow at such formate concentrations. Subsequent  
340 genome sequencing revealed that avoidance of acetate production is one of the key factors for  
341 improved growth. By-product analysis of K4e showed that this strain indeed generates acetate during  
342 growth on formate and re-assimilates excreted acetate at the late stage of the growth phase. When  
343 acetate kinase and phosphate acetyltransferase were deleted from K4e, a similar growth-profile  
344 compared to K4e2 was observed, especially with high formate concentration. While the maximal cell  
345 density previously reported was 3.5 g CDW/l and the biomass yield 2.5 g CDW/mol formate (Bang et  
346 al., 2020), the newly evolved K4e2 strain exceeded those by reaching a cell density of 8 g CDW/l and  
347 a biomass yield of 3.4 g CWD/mol formate. This finding not only exemplifies the utility of adaptive  
348 laboratory evolution but also constitutes a further step towards the industrial use of the synthetic rGly  
349 pathway. This sustainable approach to bacterial biomass production can directly find application in  
350 areas like single-cell protein or feed production. However, even more urgent but more challenging is  
351 the development of sustainable processes for value-added chemicals to provide alternatives to  
352 petroleum-based sources.

353 In order to achieve biological transformation of formate to lactate, inducible lactate dehydrogenase  
354 was implemented and the lactate assimilating quinone-dependent D-lactate dehydrogenase was  
355 deleted. When formate/formic-acid fed-batch cultivation was carried out with this strain, production of  
356 lactate was observed. We thus showed that our formatotrophic *E. coli* strain, which utilizes formate as  
357 energy and carbon source through the rGly pathway, can be further optimized, in this case by  
358 prevention of the wasteful acetate formation, and can be applied for the microbial conversion to a  
359 chemical of interest. Finally, further strain engineering to increase flux towards lactate and the  
360 establishment of an optimized bioprocess will unlock the full potential of the reductive glycine pathway



361 and hence help paving the way towards a C1-bioeconomy.

362

363 **Acknowledgements**

364 The authors thank Enrico Orsi and Hezi Tenenboim for critically reading of the manuscript. This work  
365 was funded by the Max Planck Society and by the European Union's Horizon 2020 research and  
366 innovation programme under grant agreement No. 763911 (Project eForFuel).

367

368 **Conflict of interest**

369 F. K. is cofounder of b.fab, aiming on commercialization of formate-based microbial bioproduction.

370

371 **Reference**

- 372 Baba, T., Ara, T., Hasegawa, M., Takai, Y., Okumura, Y., Baba, M., Datsenko, K. a, Tomita, M.,  
373 Wanner, B.L., Mori, H., 2006. Construction of *Escherichia coli* K-12 in-frame, single-gene  
374 knockout mutants: the Keio collection. Mol. Syst. Biol. 2, 2006.0008.  
375 <https://doi.org/10.1038/msb4100050>
- 376 Bang, J., Hwang, C.H., Ahn, J.H., Lee, J.A., Lee, S.Y., 2020. *Escherichia coli* is engineered to grow  
377 on CO<sub>2</sub> and formic acid. Nat. Microbiol. 5, 1459–1463. [https://doi.org/10.1038/s41564-020-](https://doi.org/10.1038/s41564-020-00793-9)  
378 [00793-9](https://doi.org/10.1038/s41564-020-00793-9)
- 379 Bar-Even, Arren, Flamholz, A., Noor, E., Milo, R., 2012. Thermodynamic constraints shape the  
380 structure of carbon fixation pathways. Biochim. Biophys. Acta - Bioenerg. 1817, 1646–1659.  
381 <https://doi.org/10.1016/j.bbabi.2012.05.002>
- 382 Bar-Even, A., Noor, E., Flamholz, A., Milo, R., 2013. Design and analysis of metabolic pathways  
383 supporting formatotrophic growth for electricity-dependent cultivation of microbes. Biochim.  
384 Biophys. Acta - Bioenerg. 1827, 1039–1047. <https://doi.org/10.1016/j.bbabi.2012.10.013>
- 385 Bar-Even, A., Noor, E., Milo, R., 2012. A survey of carbon fixation pathways through a quantitative  
386 lens. J. Exp. Bot. 63, 2325–2342. <https://doi.org/10.1093/jxb/err417>
- 387 Basan, M., Hui, S., Okano, H., Zhang, Z., Shen, Y., Williamson, J.R., Hwa, T., 2015. Overflow  
388 metabolism in *Escherichia coli* results from efficient proteome allocation. Nature 528, 99–104.  
389 <https://doi.org/10.1038/nature15765>
- 390 Berg, I.A., Kockelkorn, D., Ramos-Vera, W.H., Say, R.F., Zarzycki, J., Hügler, M., Alber, B.E., Fuchs,  
391 G., 2010. Autotrophic carbon fixation in archaea. Nat. Rev. Microbiol. 8, 447–460.  
392 <https://doi.org/10.1038/nrmicro2365>
- 393 Bernal, V., Castaño-Cerezo, S., Cánovas, M., 2016. Acetate metabolism regulation in *Escherichia coli*:  
394 carbon overflow, pathogenicity, and beyond. Appl. Microbiol. Biotechnol. 8985–9001.  
395 <https://doi.org/10.1007/s00253-016-7832-x>
- 396 Blattner, F.R., Goeden, M.A., Glasner, J.D., Rode, C.K., Collado-Vides, J., Mau, B., Burland, V., Rose,

- 397 D.J., Kirkpatrick, H.A., Mayhew, G.F., Plunkett, G., Bloch, C.A., Gregor, J., Davis, N.W., Riley,  
398 M., 1997. The complete genome sequence of *Escherichia coli* K-12. *Science* (80- ).
- 399 Braatsch, S., Helmark, S., Kranz, H., Koebmann, B., Jensen, P.R., 2008. *Escherichia coli* strains with  
400 promoter libraries constructed by Red/ET recombination pave the way for transcriptional fine-  
401 tuning. *Biotechniques* 45, 335–337. <https://doi.org/10.2144/000112907>
- 402 Chen, F.Y.-H., Jung, H.-W., Tsuei, C.-Y., Liao, J.C., 2020. Converting *Escherichia coli* to a Synthetic  
403 Methyloph growing solely on Methanol. *Cell* 1–14. <https://doi.org/10.1016/j.cell.2020.07.010>
- 404 Chong, L., C., C.B., Marika, Z., A., S.P., G., N.D., 2016. Water splitting–biosynthetic system with CO<sub>2</sub>  
405 reduction efficiencies exceeding photosynthesis. *Science* (80- ). 352, 1210–1213.  
406 <https://doi.org/10.1126/science.aaf5039>
- 407 Claassens, N.J., Cotton, C.A.R., Kopljar, D., Bar-Even, A., 2019. Making quantitative sense of  
408 electromicrobial production. *Nat. Catal.* 2, 437–447. <https://doi.org/10.1038/s41929-019-0272-0>
- 409 Claassens, N.J., Satanowski, A., Bysani, V.R., Dronsella, B., Orsi, E., Rainaldi, V., Yilmaz, S., Wenk,  
410 S., Lindner, S.N., 2022. Engineering the Reductive Glycine Pathway: A Promising Synthetic  
411 Metabolism Approach for C1-Assimilation BT - One-Carbon Feedstocks for Sustainable  
412 Bioproduction, in: Zeng, A.-P., Claassens, N.J. (Eds.), . Springer International Publishing, Cham,  
413 pp. 299–350. [https://doi.org/10.1007/10\\_2021\\_181](https://doi.org/10.1007/10_2021_181)
- 414 Cotton, C.A., Claassens, N.J., Benito-Vaquerizo, S., Bar-Even, A., 2020. Renewable methanol and  
415 formate as microbial feedstocks. *Curr. Opin. Biotechnol.* 62, 168–180.  
416 <https://doi.org/10.1016/j.copbio.2019.10.002>
- 417 Gassler, T., Sauer, M., Gasser, B., Egermeier, M., Troyer, C., Causon, T., Hann, S., Mattanovich, D.,  
418 Steiger, M.G., 2020. The industrial yeast *Pichia pastoris* is converted from a heterotroph into an  
419 autotroph capable of growth on CO<sub>2</sub>. *Nat. Biotechnol.* 38, 210–216.  
420 <https://doi.org/10.1038/s41587-019-0363-0>
- 421 Gleizer, S., Ben-Nissan, R., Bar-On, Y.M., Antonovsky, N., Noor, E., Zohar, Y., Jona, G., Krieger, E.,  
422 Shamshoum, M., Bar-Even, A., Milo, R., 2019. Conversion of *Escherichia coli* to Generate All  
423 Biomass Carbon from CO<sub>2</sub>. *Cell* 179, 1255-1263.e12. <https://doi.org/10.1016/j.cell.2019.11.009>

- 424 Han, L., H., O.P., G., W.D., Steve, R., Tung-Yun, W., Wendy, H., Peter, M., Yi-Xin, H., Myung, C.K.,  
425 C., L.J., 2012. Integrated Electromicrobial Conversion of CO<sub>2</sub> to Higher Alcohols. *Science* (80- ).  
426 335, 1596. <https://doi.org/10.1126/science.1217643>
- 427 He, M., Sun, Y., Han, B., 2013. Green Carbon Science: Scientific Basis for Integrating Carbon  
428 Resource Processing, Utilization, and Recycling. *Angew. Chemie Int. Ed.* 52, 9620–9633.  
429 <https://doi.org/https://doi.org/10.1002/anie.201209384>
- 430 Janssen, M., Tramper, J., Mur, L.R., Wijffels, R.H., 2003. Enclosed outdoor photobioreactors: Light  
431 regime, photosynthetic efficiency, scale-up, and future prospects. *Biotechnol. Bioeng.* 81, 193–  
432 210. <https://doi.org/https://doi.org/10.1002/bit.10468>
- 433 Kim, S., Lindner, S.N., Aslan, S., Yishai, O., Wenk, S., Schann, K., Bar-Even, A., 2020. Growth of *E.*  
434 *coli* on formate and methanol via the reductive glycine pathway. *Nat. Chem. Biol.* 16, 538–545.  
435 <https://doi.org/10.1038/s41589-020-0473-5>
- 436 Kumari, S., Tishel, R., Eisenbach, M., Wolfe, A.J., 1995. Cloning, characterization, and functional  
437 expression of *acs*, the gene which encodes acetyl coenzyme A synthetase in *Escherichia coli*. *J.*  
438 *Bacteriol.* 177, 2878–2886. <https://doi.org/10.1128/jb.177.10.2878-2886.1995>
- 439 Maki-Arvela, P., Simakova, I.L., Salmi, T., Murzin, D.Y., 2014. Production of lactic acid / lactates from  
440 biomass and their catalytic transformations to commodities. *Chem. Rev.* 114, 1909–1971.  
441 <https://doi.org/10.1021/cr400203v>
- 442 Meselson, M., Yuan, R., 1968. DNA restriction enzyme from *E. coli*. *Nature* 217, 1110–1114.  
443 <https://doi.org/10.1038/2171110a0>
- 444 Meyer, F., Keller, P., Hartl, J., Gröninger, O.G., Kiefer, P., Vorholt, J.A., 2018. Methanol-essential  
445 growth of *Escherichia coli*. *Nat. Commun.* 9. <https://doi.org/10.1038/s41467-018-03937-y>
- 446 Ogasawara, H., Ishida, Y., Yamada, K., Yamamoto, K., Ishihama, A., 2007. PdhR (pyruvate  
447 dehydrogenase complex regulator) controls the respiratory electron transport system in  
448 *Escherichia coli*. *J. Bacteriol.* 189, 5534–5541. <https://doi.org/10.1128/JB.00229-07>
- 449 Quail, M.A., Guest, J.R., 1995. Purification, characterization and mode of action of PdhR, the  
450 transcriptional repressor of the *pdhR*–*aceEF*–*lpd* operon of *Escherichia coli*. *Mol. Microbiol.* 15,

- 451 519–529. <https://doi.org/10.1111/j.1365-2958.1995.tb02265.x>
- 452 Sambrook, J., Russell, D.W., 2001. Molecular Cloning: A Laboratory Manual, Third Edition, in:  
453 Molecular Cloning: A Laboratory a Manual,.
- 454 Schwander, T., Schada von Borzyskowski, L., Burgener, S., Cortina, N.S., Erb, T.J., 2016. A synthetic  
455 pathway for the fixation of carbon dioxide in vitro. *Science* (80- ). 354.  
456 <https://doi.org/10.1126/science.aah5237>
- 457 Szenk, M., Dill, K.A., de Graff, A.M.R., 2017. Why Do Fast-Growing Bacteria Enter Overflow  
458 Metabolism? Testing the Membrane Real Estate Hypothesis. *Cell Syst.* 5, 95–104.  
459 <https://doi.org/10.1016/j.cels.2017.06.005>
- 460 Thoma, S., Schobert, M., 2009. An improved *Escherichia coli* donor strain for diparental mating.  
461 *FEMS Microbiol. Lett.* 294, 127–132. <https://doi.org/10.1111/j.1574-6968.2009.01556.x>
- 462 Thomason, L.C., Costantino, N., Court, D.L., 2007. *E. coli* Genome Manipulation by P1 Transduction.  
463 *Curr. Protoc. Mol. Biol.* <https://doi.org/10.1002/0471142727.mb0117s79>
- 464 Wang, Y., Huang, Y., Wang, J., Cheng, C., Huang, W., Lu, P., Xu, Y.N., Wang, P., Yan, N., Shi, Y.,  
465 2009. Structure of the formate transporter FocA reveals a pentameric aquaporin-like channel.  
466 *Nature* 462, 467–472. <https://doi.org/10.1038/nature08610>
- 467 Wei, L., Juan, D., Tobias, W., Elke, G.-S., A., A.S.L., Oliver, E., 2011. pH-Dependent Gating in a FocA  
468 Formate Channel. *Science* (80- ). 332, 352–354. <https://doi.org/10.1126/science.1199098>
- 469 Wiechert, M., Beitz, E., 2017. Mechanism of formate–nitrite transporters by dielectric shift of substrate  
470 acidity. *EMBO J.* 36, 949–958. <https://doi.org/10.15252/embj.201695776>
- 471 Wolfe, A.J., 2005. The Acetate Switch. *Microbiol. Mol. Biol. Rev.* 69, 12–50.  
472 <https://doi.org/10.1128/mnbr.69.1.12-50.2005>
- 473 Wong, T.S., 2014. Carbon Dioxide Capture and Utilization using Biological Systems: Opportunities  
474 and Challenges. *J. Bioprocess. Biotech.* 04. <https://doi.org/10.4172/2155-9821.1000155>
- 475 Yishai, O., Bouzon, M., Döring, V., Bar-Even, A., 2018. In vivo assimilation of one-carbon via a  
476 synthetic reductive glycine pathway in *Escherichia coli*. *ACS Synth. Biol.*

477 <https://doi.org/10.1021/acssynbio.8b00131>

478 Yishai, O., Lindner, S.N., Gonzalez de la Cruz, J., Tenenboim, H., Bar-Even, A., 2016. The formate  
479 bio-economy. *Curr. Opin. Chem. Biol.* 35, 1–9. <https://doi.org/10.1016/j.cbpa.2016.07.005>

480 Zelcbuch, L., Antonovsky, N., Bar-Even, A., Levin-Karp, A., Barenholz, U., Dayagi, M., Liebermeister,  
481 W., Flamholz, A., Noor, E., Amram, S., Brandis, A., Bareia, T., Yofe, I., Jubran, H., Milo, R.,  
482 2013. Spanning high-dimensional expression space using ribosome-binding site combinatorics.  
483 *Nucleic Acids Res.* 41. <https://doi.org/10.1093/nar/gkt151>

484 Zhu, X.-G., Long, S.P., Ort, D.R., 2010. Improving Photosynthetic Efficiency for Greater Yield. *Annu.*  
485 *Rev. Plant Biol.* 61, 235–261. <https://doi.org/10.1146/annurev-arplant-042809-112206>

486

487